

AD-A121 425

UNIFORM LASER ABLATIVE ACCELERATION OF TARGETS AT
10(14)W/CM(2)(U) NAVAL RESEARCH LAB WASHINGTON DC
S P OBENSCHAIN ET AL. 30 SEP 82 NRL-MR-4926

171

UNCLASSIFIED

F/G 20/5

NL

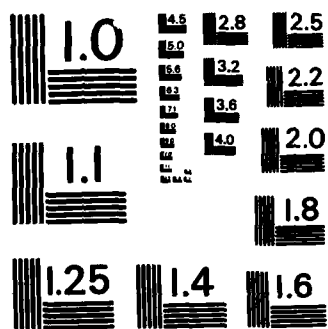


END

FILMED

+

DTIC



MICROCOPY RESOLUTION TEST CHART
NATIONAL BUREAU OF STANDARDS-1963-A

AD A 121 425

REPORT DOCUMENTATION PAGE		READ INSTRUCTIONS BEFORE COMPLETING FORM
1. REPORT NUMBER NRL Memorandum Report 4926	2. GOVT ACCESSION NO.	3. RECIPIENT'S CATALOG NUMBER
4. TITLE (and Subtitle) UNIFORM LASER ABLATIVE ACCELERATION OF TARGETS AT 10^{14} W/cm ²	5. TYPE OF REPORT & PERIOD COVERED	
	6. PERFORMING ORG. REPORT NUMBER	
7. AUTHOR(s) S. P. Obenschain, R. R. Whitlock, E. A. McLean, B. H. Ripin, R. H. Price,* D. W. Phillion,* E. M. Campbell,* M. D. Rosen,* and J. M. Auerbach*	8. CONTRACT OR GRANT NUMBER(s)	
9. PERFORMING ORGANIZATION NAME AND ADDRESS Naval Research Laboratory Washington, DC 20375	10. PROGRAM ELEMENT, PROJECT, TASK AREA & WORK UNIT NUMBERS DOE AI08-79DP 40092 (172) 47-0859-0-2	
11. CONTROLLING OFFICE NAME AND ADDRESS U.S. Department of Energy Washington, DC 20545	12. REPORT DATE September 30, 1982	
	13. NUMBER OF PAGES 8	
14. MONITORING AGENCY NAME & ADDRESS (if different from Controlling Office)	15. SECURITY CLASS. (of this report) UNCLASSIFIED	
	15a. DECLASSIFICATION/DOWNGRADING SCHEDULE	
16. DISTRIBUTION STATEMENT (of this Report) Approved for public release; distribution unlimited.		
17. DISTRIBUTION STATEMENT (of the abstract entered in Block 20, if different from Report)		
18. SUPPLEMENTARY NOTES *Lawrence Livermore National Laboratory, Livermore, CA		
19. KEY WORDS (Continue on reverse side if necessary and identify by block number) Laser-fusion Ablation Laser-plasma Ablation pressure		
20. ABSTRACT (Continue on reverse side if necessary and identify by block number) We present the first detailed investigations of the ablative acceleration of planar targets while simultaneously using high irradiance (10^{14} W/cm ²), large focal diameters (1 mm) and long laser pulse duration (3 nsec). Included are measurements of target preheat, ablation pressures and uniformity achieved under these conditions. Targets were accelerated to high velocities with velocity profile uniformity approaching that required for high gain pellet implosions.		

DD FORM 1473
1 JAN 73EDITION OF 1 NOV 65 IS OBSOLETE
S/N 0102-014-6601

SECURITY CLASSIFICATION OF THIS PAGE (When Data Entered)

UNIFORM LASER ABLATIVE ACCELERATION OF TARGETS AT 10^{14} W/cm²

A high gain pellet implosion requires that the pellet shell be uniformly and efficiently accelerated to velocities above 150 km/sec with controlled levels of preheat.^{1,2} Experiments at NRL have modelled the early stages of a pellet implosion through studies of ablatively accelerated planar targets by direct illumination with a 500-J, 3-nsec, Nd-glass laser.³⁻⁶ These experiments have studied the feasibility of simultaneously achieving the uniform and efficient ablative acceleration of matter required for pellet fusion while maintaining low levels of preheat. Here we present results from similar experiments using the LLNL Shiva laser at much higher laser energies and higher irradiances. This allowed us to probe parameter regimes closer to the fusion reactor scenario and explore both the hydrodynamic properties of the accelerated foils and whether deleterious plasma instabilities appear which could reduce absorption and increase preheat.

Actual high gain (fusion reactor) pellets will likely require intensities of at least 10^{14} W/cm² (at 1 μ m) in order to: (1) achieve minimum pressures (about 10-20 Mbar) required to drive moderate aspect ratio pellets;⁷ and (2) to obtain sufficiently large absorption-ablation layer separations to get adequate lateral smoothing^{8,9} of laser nonuniformities over dimensions comparable to the radius of high-gain pellets (several mm).¹ In this paper we discuss the observed physics associated with planar target acceleration and preheat at intensities near 10^{14} W/cm². The present experimental conditions are distinguished from other studies at the same irradiance in that the focal spot diameter was large (1 mm) and the laser pulse was relatively long 3-3.5 nsec. These conditions allow the formation of long scalelength blowoff plasmas which would also be present with the large pellets envisioned for high energy gain.

For this experiment ten beams of the Shiva-laser¹⁰ (3-3.5 nsec FWHM, 3-4 kJ, 1.06 μ m) were focused to a 1 mm diameter spot (90% energy content) and overlapped onto carbon foil targets. The carbon foils were typically 10 μ m thick and significantly wider (2.5 mm width) than the focal spot in order to isolate the cooler rear side of the target foils from the laser irradiated (front) side. Arrays of diagnostics monitored the laser target interaction including the absorption fraction, scattered light distribution, the yield and spectrum of both the $3/2\omega_0$ and stimulated Raman scattered light, suprathermal x-ray production, and optical emission from the rear surface of the target. The dynamics of the accelerated target foil was determined using streaked x-ray shadowgraphy,^{11,12} while the double-foil technique was used to measure the velocity profile uniformity.⁵

Figure 1(a) shows a streaked x-ray shadowgraph of a target ablatively accelerated by a 3.2 nsec FWHM, 3 kJ laser pulse ($I_{\text{peak}} \sim 1.1 \times 10^{14}$ W/cm²) to about 10^7 cm/sec. The backlighting x-rays, produced by a Pd target illuminated by 8 beams of the Shiva laser, are energetic enough (2.8-3.2 keV) to penetrate to the denser regions of the accelerated targets ($\rho \geq 0.1 \rho_{\text{solid}}$). The image of the target was focused onto an x-ray streak camera with the slit parallel to the accelerated target's direction. Spatial and temporal resolution were 6-7 μ m and 20 psec respectively.¹¹ Relatively thick targets were chosen for these studies so that the fraction of mass ablated was small, making target accelerations nearly proportional to the ablation pressures. Figure 1(b) shows the experimentally determined evolution of the target velocity as compared to values calculated using experimentally measured⁶ scaling laws for mass ablation rates and pressures. ($P \propto I_{\text{ABS}}^{0.8}$, $\dot{m} \propto I_{\text{ABS}}^{0.6}$ where I_{ABS} is the absorbed irradiance with $P/\dot{m} = 3.6 \times 10^7$ cm/sec at $P = 10^{12}$ dynes/cm².) The best fit to the observed velocity, which is shown



by Ood
and/or
Special
A

in the figure, was attained at a peak pressure of 6 Mbar with about 20% of the mass ablated. Due to the small ablated mass, this pressure result is relatively insensitive to any errors in estimates of the mass ablation rate. We believe the maximum error in the above pressure is $\pm 15\%$. Light diodes found that $60 \pm 6\%$ of the incident light was absorbed, indicating the peak absorbed irradiance was about 6×10^{13} W/cm² (constant absorptivity and nominal spot size are assumed). Extrapolations of planar target experiments at lower absorbed irradiances⁶ and 1-dimensional hydrodynamic code results would predict a somewhat higher peak pressure of about 9 Mbar at this absorbed irradiance. The low observed pressure is at least partially due to lateral energy flow in the blow-off plasma which cools the irradiated portion of the foil targets and heats the periphery. This lateral energy flow also smooths laser nonuniformities and is discussed in detail below. Another contributing effect may be an increase in the focal spot size at the critical layer due to plasma expansion in the converging (effective f/1) laser beam cluster. Two-dimensional calculations using the LASNEX hydrodynamic code,¹³ which accounts for such effects, predicted peak pressures of 5 Mbar for the absorbed energies encountered, in good agreement with the pressure observed.

The velocity profiles across the accelerated targets were determined using the double-foil technique. This method involves placing a second foil (impact foil) parallel to and (200 μ m) behind the first. Nonuniformities in the impact time of the accelerated foil are monitored by observations of the light emitted from the impact foil's rear surface. Figure 2(b) shows a streak record of light emitted from the rear of the impact foil upon collision by a carbon foil ablatively accelerated at 10^{14} W/cm² to about 10^7 cm/sec. X-ray shadowgraphy (Fig. 2(a)) shows that the collision occurred near the end of the laser pulse. Given the measured target velocity and the foil spacing, one can calculate the velocity nonuniformities of the target from the differences in impact times of different sections of the accelerated target. The nonuniformities can be resolved into an 8% tilt across the central 1 mm of the target plus modulations with 7% peak-to-valley amplitude ($V_{\max}/V_{\min}-1$). When sampled over short scalelengths (50-200 μ m) in the central 800 μ m region irradiated by the laser, the observed peak-to-valley velocity nonuniformity is only 5%. The resolution limit for velocity nonuniformities due to limited temporal resolution of the streak camera is about 3%. This resolution limit is manifested in granularity of the streak photographs and thus the actual target uniformity over short scalelengths may be better than 5%.

Factors which can cause velocity nonuniformities include target mass nonuniformities, laser irradiation nonuniformities and hydrodynamic instabilities. Carbon foils typical of those used in the experiment have mass thickness nonuniformities of less than 2% across the focal diameter and thus target mass nonuniformities are not thought to be a significant factor. The laser beams employed were defocused and overlapped to minimize the irradiation nonuniformities. Each beam has intensity nonuniformities with typical peak-to-valley amplitude of about 2 to 1 (scale length range from ~ 0.1 to 0.5 of the beam diameter) in the near field. Ignoring phase nonuniformity contributions, this would produce similar amplitude modulations at the 1 mm focus. Averaging due to beam overlap should decrease the irradiation nonuniformity of the target by about the square root of the number of beams ($10^{-1/2}$). However, no actual measurement exists at the target plane. We estimate the illumination nonuniformities on target have typical peak to valley amplitude of about 30%. The observed short scalelength velocity nonuniformities are at least a factor of 4 to 6 smaller than the *estimated* intensity nonuniformity indicating significant lateral smoothing.

One-dimensional hydrodynamic calculations¹⁴ predict that the absorption-to-ablation separation in steady state should be near 1 mm at 10^{14} W/cm². The blow-off plasma divergence and limited laser pulse length prevents one from attaining this large a separation in our experiment. Two-dimensional LASNEX calculations for the conditions of the experiment predict separations of 200-300 μ m. The observed lateral smoothing appears to be consistent with this calculated separation. The lateral heat conduction, which helps smooth out beam variations, should also be manifested by a larger region of the target foil being accelerated than the laser focal spot. The double-foil collision data in fact show that an area 2.2 times that of the laser focal spot is accelerated to 60% of the peak target velocity. This result was also in agreement with LASNEX calculations.

For the fusion application, low target preheat is essential. In these experiments, the target preheat was monitored by measuring the rear surface brightness temperature⁴ (at $\sim 4200 \text{ \AA}$) using a calibrated optical streak camera. The streak camera images show that the heating is initially confined to the center laser illuminated region indicating that little energy is being transported around the target foils. The time resolved rear surface temperatures for single and double foil targets are given in Fig. 3. The accelerated carbon target thickness was $11 \text{ }\mu\text{m}$ in both cases while an $8\text{-}\mu\text{m}$ thick carbon impact foil was employed for the double foil target. The rear surface of the single foil exhibits a sudden temperature rise soon after initiation of the laser pulse. LASNEX simulations indicate this early heating is due to shocks produced by the leading edge of the laser pulse. Absolute x-ray spectra indicate that about 3% of the absorbed laser light is deposited in a 10-keV suprathermal electron distribution.¹⁵ Deposition of these hot electrons in the single foil can account for the remainder of the observed heating to a 15-eV peak temperature after the initial shocks. The hot electrons can also account for the observed preheat of the impact foil prior to collision. A detailed analysis of the interaction which may be producing these hot electrons will be presented elsewhere.¹⁵ The presence of copious $3/2 \omega_0$ emission but absence of significant raman scattered light suggest that the two-plasmon decay instability may be involved. The rear surface of the impact foil is further heated after collision due to high pressure shocks. Temperatures of up to 60 eV were observed for the case of a $17\text{-}\mu\text{m}$ thick C foil irradiated at $2 \times 10^{14} \text{ W/cm}^2$ and impacting at about 60 km/sec. Details of this phenomenon will also be presented elsewhere.

In conclusion, the results of this planar target series at 10^{14} W/cm^2 are the expected extrapolation of lower irradiance studies in regard to ablation pressures and symmetrization, provided that finite focal spot size effects are accounted for. The target velocity uniformity achieved in this experiment was a factor of 2 better than that attained in earlier single beam experiments at lower irradiances⁵ and perhaps approaches that required for high gain implosions. Minimum uniformities of a few percent are thought to be required.⁷ Hot electrons were found to be an important preheat phenomenon for thin targets in contrast to lower irradiance studies.⁴ However, the observed hot electrons at 10^{14} W/cm^2 are not energetic enough to penetrate the much thicker walled ($\Delta r > 100 \text{ }\mu\text{m}$) targets envisioned for high-gain pellets. The results were thus encouraging for the direct illumination approach to inertial fusion through the intensities and plasma scalelengths encountered. However, it should be noted that the longer laser pulse lengths ($> 10 \text{ nsec}$) required,^{1,2} and higher irradiances desired for reactor systems will produce longer scalelength plasmas than encountered here; testing the resulting coupling physics and symmetrization awaits more energetic laser systems.

We thank Morton Fink, O. Barr, J. Stamper, J. Grun, S. Bodner, J. Lindl, the Shiva crew, and the LLNL target fabrication group for their support in these experiments. This work was supported by the U.S. Department of Energy.

REFERENCES

1. John H. Nuckolls, et al., in Proceedings of the European Conference on Laser Interaction with Matter, Oxford, England, 1977 (unpublished).
2. J. Lindl, Report UCRL-80104 (Sept. 1977).
3. B.H. Ripin, et al., Phys. Fluids **23**, 1012 (1980).
4. E.A. McLean, et al., Phys. Rev. Lett. **45**, 1246 (1980).
5. S.P. Obenshain, J. Grun, B.H. Ripin and E.A. McLean, Phys. Rev. Lett. **46**, 1402 (1981) and **48**, 709 (1982).
6. J. Grun, R. Decoste, B.H. Ripin and J. Gardner, Appl. Phys. Lett. **39**, 545 (1981).

7. S.E. Bodner, J. Fusion Energy, 1, 221 (1981).
8. J.H. Gardner and S.E. Bodner, Phys. Rev. Lett. 47, 1137 (1981).
9. C.E. Max, J.D. Lindl, W.C. Mead, LLNL Report UCRL-86715 Rev. 1, February 8, 1982.
10. D.R. Speck, et al., IEEE J. Quantum Elect. 17, 1599 (1981).
11. R.H. Price, M.D. Rosen, D.L. Banner and J.R. Zickuhr, LLNL Laser Program Annual Report, 7-44 (1980).
12. A. Raven et al., Appl. Phys. Lett., 40, 776 (1982).
13. G.B. Zimmerman, Lawrence Livermore National Laboratory Report No. UCRL-74811 (1973); and W.L. Kruer, Comments Plasma Phys. 2, 85 (1975).
14. W.M. Manheimer, D.G. Colombant and J.H. Gardner, NRL Memorandum Report 4644 (1981).
15. E.M. Campbell, et al., 1982 IEEE International Conference on Plasma Science, Ottawa, Canada. (To be published).

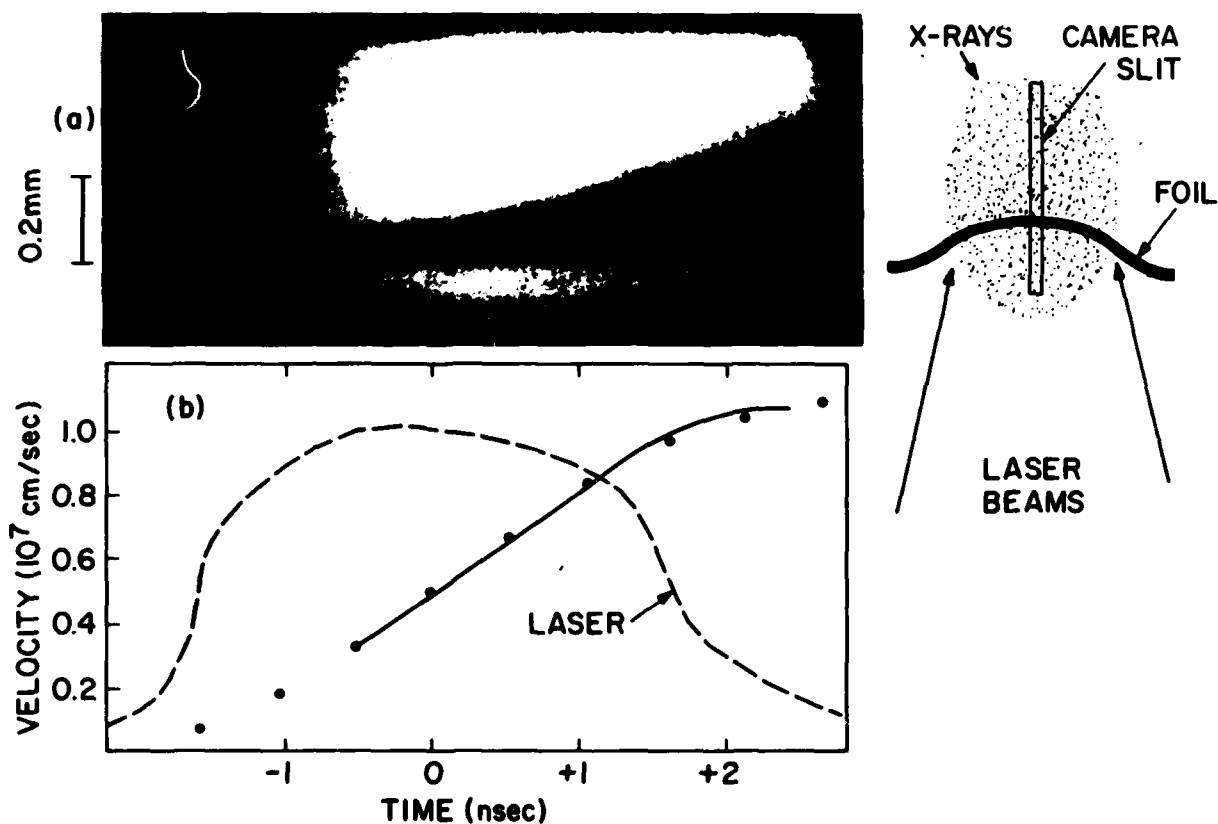


Fig. 1 — (a) Streaked x-ray shadowgraph of an accelerated C foil target whose initial areal mass was 2.1 mg/cm^2 ; (b) the velocity evolution of target determined from the x-ray shadowgraph (solid line). The closed circles are the calculated velocity using the scaling laws described in the text.

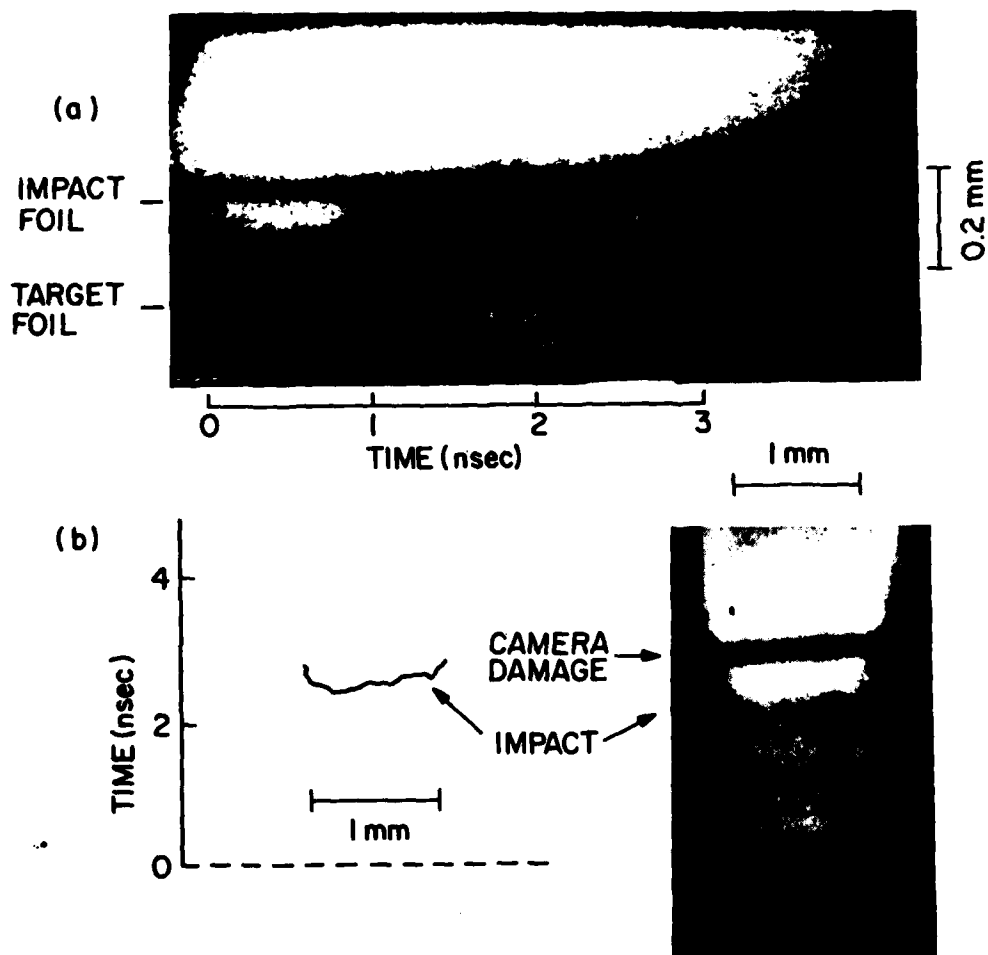


Fig. 2 — (a) Streaked x-ray shadowgraph of the collision of an accelerated foil target with an impact foil located $200\text{ }\mu\text{m}$ behind; (b) the photograph is an optical streak camera record of light emission from the rear of an impact foil struck by a laser accelerated target. A contour plot of this light emission (at 40% of peak) is given to the left. The spatial resolution is $50\text{ }\mu\text{m}$. Zero on the time scales is the peak of the laser pulse.

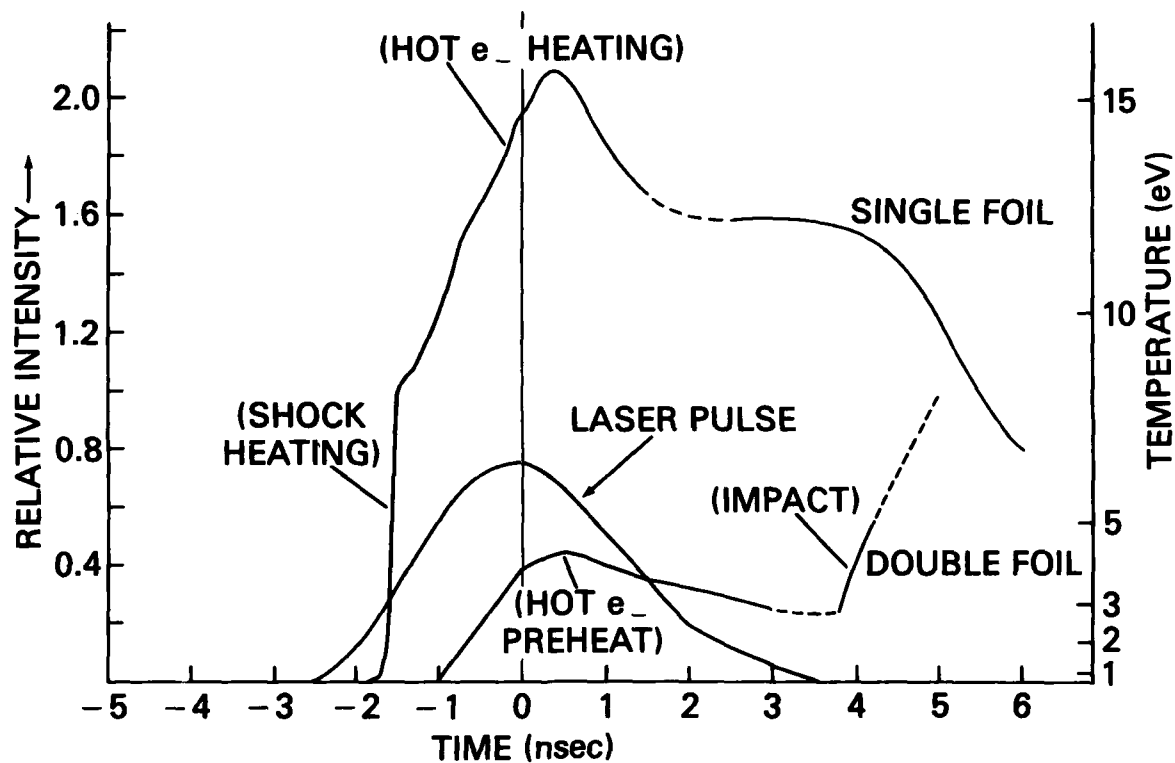


Fig. 3 — Time evolution of the brightness temperature of the rear surface of an accelerated single foil, and the impact foil of a double foil target. The absolute calibration of the emissivity from which the temperatures were calculated is accurate to within a factor of two for these measurements. This corresponds to an accuracy for the temperature determination of a factor of 2 for $T > 2$ eV, with improved accuracy at temperatures below 2 eV.